Supplementary Information (SI) for Materials Horizons.
This journal is © The Royal Society of Chemistry 2025

Supplementary Information for

Pseudo Lattice-Breathing Driven Valley Switching in 2D Ferromagnetic Lattices

Tight-binding Model

In this system, consisting of a magnetic triangular sublattice (A) and a hexagonal sublattice (B), nearest-neighbor (NN) hopping occurs between the nonequivalent A and B sites, while next-nearest-neighbor (NNN) hopping takes place within the A or B sublattice.

To describe the valley physics of the lattice, we construct an effective tight-binding model for characterizing the low-energy band dispersions near the Fermi level:

$$H(k)=\begin{pmatrix} H_{hop,\uparrow}(k) & 0 \\ 0 & H_{hop,\uparrow}(k) \end{pmatrix}+\begin{pmatrix} H_{soc,\uparrow} & 0 \\ 0 & H_{soc,\uparrow} \end{pmatrix}-\begin{pmatrix} M_A I & 0 & 0 & 0 \\ 0 & M_B I & 0 & 0 \\ 0 & 0 & -M_A I & 0 \\ 0 & 0 & 0 & -M_B I \end{pmatrix} \#(1)$$

where H_{hop} involves the NN and NNN hopping terms. H_{soc} is the on-site SOC term, the up and down arrows indicate the spin-up and spin-down channels, respectively. H_M is the magnetic exchange field term in the lattice. I is a unit matrix. and M_A and M_B are the applied exchange field strengths on the A site and B site, respectively.

The hopping terms for the spin-up and spin-down channels can both be expressed as ($H_{hop\uparrow}=H_{hop\downarrow}$):

$$H_{hop\uparrow/\downarrow}=\begin{bmatrix} h11 & h12 & h13 & h14 \\ h21 & h22 & h23 & h24 \\ h31 & h32 & h33 & h34 \\ h41 & h42 & h43 & h44 \end{bmatrix} \#(2)$$

With the A and B sites of the honeycomb lattice occupied by different atom types that also have distinct orbital types (d_{xy}/d_{x2-y2} at A site and p_x/p_y at B site) and parameters, the matrix elements $E_{i,j}(\vec{r}_{n,n}{}') = \langle n,i|H|n',j\rangle$ for the tight-binding model are derived using the Slater-Koster overlap integral method. The various integrals are treated as fitting parameters such that the TB model matches accurate calculations at high-symmetry points in the Brillouin zone. The LCAO method is then employed for interpolating band structures across the entire Brillouin zone. The parameters used in this article are as follows：

$$
\begin{aligned}
E_{x,x} &= l^2 t_{pp\sigma} + (1-l^2) t_{pp\pi} \\
E_{x,y} &= lm t_{pp\sigma} - lm t_{pp\pi} \\
E_{x,x^2-y^2} &= \frac{\sqrt{3}}{2} l(l^2-m^2) V_{pd\sigma} + l(1-l^2+m^2) V_{pd\pi} \\
E_{x,xy} &= \sqrt{3} l^2 m V_{pd\sigma} + m(1-2l^2) V_{pd\pi} \\
E_{y,y} &= m^2 V_{pp\sigma} + (1-m^2) V_{pp\pi} \\
E_{y,xy} &= \sqrt{3} m^2 n V_{pd\sigma} + l(1-2m^2) V_{pd\pi} \\
E_{y,x^2-y^2} &= \frac{\sqrt{3}}{2} m(l^2-m^2) V_{pd\sigma} - m(1+l^2-m^2) V_{pd\pi} \\
E_{xy,xy} &= 3l^2 m^2 t_{dd\sigma} + (l^2+m^2-4l^2m^2) t_{dd\pi} + (n^2+l^2m^2) t_{dd\delta} \\
E_{x^2-y^2,x^2-y^2} &= \frac{3}{4(l^2-m^2) t_{dd\sigma}} + \left[l^2+m^2-(l^2-m^2)^2\right] t_{dd\pi} + \left[n^2 + \frac{(l^2-m^2)^2}{4}\right] t_{dd\delta} \\
E_{xy,x^2-y^2} &= \frac{3}{2} lm(l^2-m^2) t_{dd\sigma} + 2lm(m^2-l^2) t_{dd\pi} + \left[\frac{lm(l^2-m^2)}{2}\right] t_{dd\delta}
\end{aligned} \quad \#(3)
$$

The $t_{pp\pi}$, $t_{pp\sigma}$, $t_{dd\pi}$, $t_{dd\sigma}$ and $t_{dd\delta}$ (the NNN hopping parameters), and $t_{pd\sigma}$ and $t_{pd\pi}$ (the NN hopping parameters), which correspond to the π, σ and δ bonds formed by p_x/p_y and d_{xy}/d_{x2-y2} orbitals. The direction cosines l, m, n represent the projections of the interatomic vector along the x, y, and z directions. For the system studied here, the direction cosines for lattice vectors a_1 and a_2 are (l, m, n) = (√3/2, -1/2, 0) and (√3/2, 1/2, 0), respectively. Thus, each specific matrix element can be obtained:

$$
\begin{aligned}
h11 &= \varepsilon_d + 2t_{dd\pi}cos(\sqrt{3}k_y) + \frac{1}{8}(9t_{dd\sigma} + 4t_{dd\pi} + 3t_{dd\delta})(cos(\frac{3}{2}k_x - \frac{\sqrt{3}}{2}k_y) + cos(\frac{3}{2}k_x + \frac{\sqrt{3}}{2}k_y)), \\
h12 &= -\frac{\sqrt{3}}{8}(3t_{dd\sigma} - 4t_{dd\pi} + t_{dd\delta})(cos(\frac{3}{2}k_x - \frac{\sqrt{3}}{2}k_y) - cos(\frac{3}{2}k_x + \frac{\sqrt{3}}{2}k_y)), \\
h13 &= (\frac{3}{8}t_{pd\sigma} + \frac{\sqrt{3}}{4}t_{pd\pi})(e^{i(-\frac{1}{2}k_x + \frac{\sqrt{3}}{2}k_y)} - e^{i(-\frac{1}{2}k_x - \frac{\sqrt{3}}{2}k_y)}), \\
h14 &= \frac{\sqrt{3}}{2}t_{pd\sigma}e^{ik_x} + (\frac{\sqrt{3}}{8}t_{pd\sigma} - \frac{3}{4}t_{pd\pi})(e^{i(-\frac{1}{2}k_x + \frac{\sqrt{3}}{2}k_y)} + e^{i(-\frac{1}{2}k_x - \frac{\sqrt{3}}{2}k_y)}), \\
h22 &= \varepsilon_d + \frac{1}{2}(3t_{dd\sigma} + t_{dd\delta})cos(\sqrt{3}k_y) + \frac{1}{8}(3t_{dd\sigma} + 12t_{dd\pi} + t_{dd\delta})(cos(\frac{3}{2}k_x - \frac{\sqrt{3}}{2}k_y) + cos(\frac{3}{2}k_x + \frac{\sqrt{3}}{2}k_y)), \\
h23 &= t_{pd\pi}e^{ik_x} + (-\frac{3\sqrt{3}}{8}t_{pd\sigma} + \frac{1}{4}t_{pd\pi})(e^{i(-\frac{1}{2}k_x + \frac{\sqrt{3}}{2}k_y)} + e^{i(-\frac{1}{2}k_x - \frac{\sqrt{3}}{2}k_y)}), \\
h24 &= (-\frac{3}{8}t_{pd\sigma} - \frac{\sqrt{3}}{4}t_{pd\pi})(e^{i(-\frac{1}{2}k_x + \frac{\sqrt{3}}{2}k_y)} - e^{i(-\frac{1}{2}k_x - \frac{\sqrt{3}}{2}k_y)}), \\
h33 &= \varepsilon_p + 2t_{pp\pi}cos(\sqrt{3}k_y) + (\frac{3}{2}t_{pp\sigma} + \frac{1}{2}t_{pp\pi})(cos(\frac{3}{2}k_x - \frac{\sqrt{3}}{2}k_y) + cos(\frac{3}{2}k_x + \frac{\sqrt{3}}{2}k_y)), \\
h34 &= \frac{\sqrt{3}}{2}(t_{pp\pi} - t_{pp\sigma})(cos(\frac{3}{2}k_x - \frac{\sqrt{3}}{2}k_y) - cos(\frac{3}{2}k_x + \frac{\sqrt{3}}{2}k_y)), \\
h44 &= \varepsilon_p + 2t_{pp\sigma}cos(\sqrt{3}k_y) + (\frac{1}{2}t_{pp\sigma} + \frac{3}{2}t_{pp\pi})(cos(\frac{3}{2}k_x - \frac{\sqrt{3}}{2}k_y) + cos(\frac{3}{2}k_x + \frac{\sqrt{3}}{2}k_y)), \\
h21 &= h12, h43 = h34, h31 = -h13^*, h32 = -h23^*, h41 = -h14^*, h42 = -h24^*
\end{aligned} \quad (4)
$$

Here, the ε_p and ε_d are respectively the on-site energy for p_x/p_y and d_{xy}/d_{x2-y2} orbitals.

For the different spin subspaces, the on-site SOC is written as a 4×4 matrix:

$$H_{soc\uparrow/\downarrow} = s \cdot \begin{bmatrix} 0 & -\lambda_A i & 0 & 0 \\ \lambda_A i & 0 & 0 & 0 \\ 0 & 0 & 0 & 2\lambda_B i \\ 0 & 0 & -2\lambda_B i & 0 \end{bmatrix} \#(5)$$

Where λ_A and λ_B is the atomic SOC strength of the A site and B site, respectively. $s = \pm 1$ represent the spin-up and spin-down components, respectively. The details of the specific values are listed in Table S1and Table S2.

Table S1. The Slater-Koster overlap integral method parameters for the band dispersions near the Fermi level. All the parameters are in units of eV.

ε_p	ε_d	$t_{pp\sigma}$	$t_{pp\pi}$	$t_{pd\sigma}$	$t_{pd\pi}$	$t_{dd\sigma}$	$t_{dd\pi}$	$t_{dd\delta}$
-0.35	0.54	-0.04	0.07	0.01	-0.05	-0.15	0.02	0.3

Table S2. The tight-binding model parameters for the band dispersions near the Fermi level. All the parameters are in units of eV.

λ_A	λ_B	M_A	M_B	s
0.15	0.18	0.02	0.02	1

Fig. S1 (a) ferromagnetic (FM), two antiferromagnetic (AFM), (b) G-AFM, (c) C-AFM, and (d) ferrimagnetic (FIM) configurations of EuGe2 monolayer. J presents the magnetic coupling parament between the nearest neighboring (NN) Eu atoms.

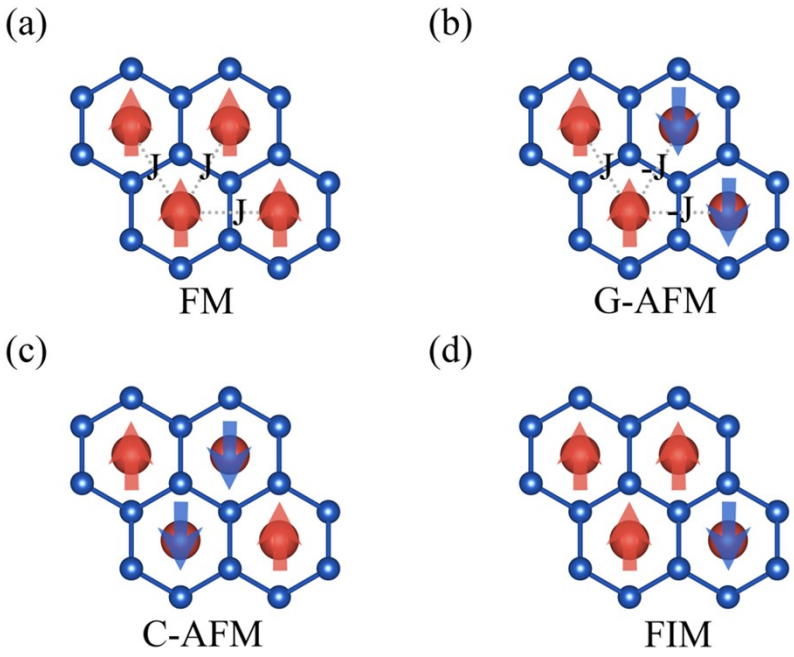
(a)
J
J
J
FM
(b)
J
-J
-J
G-AFM
(c)
C-AFM
(d)
FIM